Core Modified *meso*-Aryl Corrole: First Examples of Cu^{II}, Ni^{II}, Co^{II} and Rh^{I} Complexes

Bashyam Sridevi,[a] Seenichamy Jeyaprakash Narayanan,[a] Tavarekere K. Chandrashekar,*[a] Ulrich Englich,[b] and Karin Ruhlandt-Senge[b]

Dedicated to Professor P. Natarajan on the occasion of his 60th birthday

Abstract: A variety of metal complexes of 5,10,15-triphenyl-21-monooxa-corrole **4** have been investigated. This monooxa corrole, where one of the pyrrole ring is replaced by a furan moiety, is synthesized by the $\alpha-\alpha$ coupling reaction of 16-oxa tripyrrane and dipyrromethane. The single crystal X-ray structure of **4** indicates only small deviation of the inner-core heteroatoms from planarity and this macrocycle arrange themselves into a columnar structure. Insertion of metals further flattens the corrole framework. Specifically, oxacorrole **4** binds to Ni^{II}, Cu^{II}, and Co^{II} with the participation of all heteroatoms in the coordination. However, Rh^{I} ion binds to only one imino and one amino nitrogen of the macrocycle. The bond angles at the metal center in the Ni^{II} and Rh^{I} complexes reveal square planar geometry completed by two CO molecules for Rh^{I}. The EPR spectra of the paramagnetic that Cu^{II} and Co^{II} complexes display significant decreases in the metal hyperfine couplings compared with the corresponding porphyrin complexes. The presence of superhyperfine coupling in the Cu^{II} complex suggests delocalization of unpaired electron density into the ligand orbitals. Electrochemical studies reveal easier oxidations and harder reductions relative to the corresponding porphyrin derivatives while, the metallated derivatives did not show their characteristic metal reductions due to the high energy of their LUMO.

Keywords: core-modified corroles · macrocycles · metallocorroles · porphyrinogens

Introduction

A corrole macrocycle is a cyclic tetrapyrrole with a direct pyrrole–pyrrole link and is related to the corrin macrocycle which is involved in biosynthetic pathway of vitamin B_{12}.[1] The corrole ring can be considered as being a formal intermediate in nature between porphyrin and corrin.[2] Structurally, the corrole skeleton can be viewed as by removing one of the *meso* carbons from the porphyrin ring. Both porphyrin and corrole are aromatic 18π-systems, which exhibit intense absorptions in the visible region and share many similar properties. Inspite of this similarity, the chemistry of corroles are not as well developed as their porphyrin analogues because of the difficulties encountered in the synthesis of corroles. Johnson and co-workers were first to report the synthesis of metallo corroles by a ring closure reaction of a metallo-dibromo-bi(dipyrryl methane) in the presence of formaldehyde.[3] They were also successful in synthesis of mesooxa[4] and thiacorroles[5] from the corresponding metallo linear tetrapyrroles. Later, Broadhurst and co-workers[6] designed a rational "2+2" approach for the synthesis of a variety of normal and heteroatom containing metallo corroles. More recently, Vogel and co-workers[7] have reported the synthesis of tetraoxa corrole dication by a cyclo condensation of hydroxy methyl substituted mono furan precursor. However, most of the synthesis described above were confined to β-substituted corroles.

The first *meso* aryl substituted corrole was reported only in 1993.[8a] Later, a direct synthesis of triphenyl corrole was reported by a self-condensation of a mono pyrrolic unit[8b] to give a porphyrinogen which on reaction with Co^{II} salt and triphenyl phosphine underwent a ring contraction to give Co^{III} corrole. The mechanism of ring contraction is not established yet. In 1996, Rose and co-workers isolated *meso*-aryl corrole as byproduct of the reaction in about 5% yield.[9] In 1999, three groups around the globe independently reported a

[a] Prof. T. K. Chandrashekar, B. Sridevi, S. Jeyaprakash Narayanan
Department of Chemistry, Indian Institute of Technology
Kanpur-208 016 (India)
Fax: (+91 512) 597436/590260/590007
E-mail: tkc@iitk.ac.in

[b] U. Englich, Prof. K. Ruhlandt-Senge
Department of Chemistry, Syracuse University
Syracuse, New York 13244 (USA)

Supporting information for this contribution is available on the WWW under http://www.wiley-vch.de/home/chemistry/

0947-6539/00/0614-2554 $ 17.50+.50/0 *Chem. Eur. J.* **2000**, *6*, No. 14

direct synthesis of *meso*-aryl free-base corroles. Gross et al.[10] and Paolesse and coworkers[11] isolated 5,10,15-triaryl corroles from reaction of pyrrole and aromatic aldehydes under different conditions, while Chandrashekar and coworkers[12] isolated 5,10,15-triphenyl-21-monooxa corrole **4** as a byproduct in a 3+2 coupling reaction of appropriate precursors. In continuation of this work, in this paper we wish to report different metal derivatives of monooxa-corrole **4** and their properties. It has been shown that the monooxa corrole reacts with divalent metal salts to form authentic four coordinate complexes, while its reaction with Rh^{I} precursor gives an complex in which only one amino and one imino nitrogen of the corrole coordinates to the metal. ESR studies reveal well resolved spectra for both Cu^{II} and Co^{II} corrole complexes, further confirming the divalent nature of the metals.

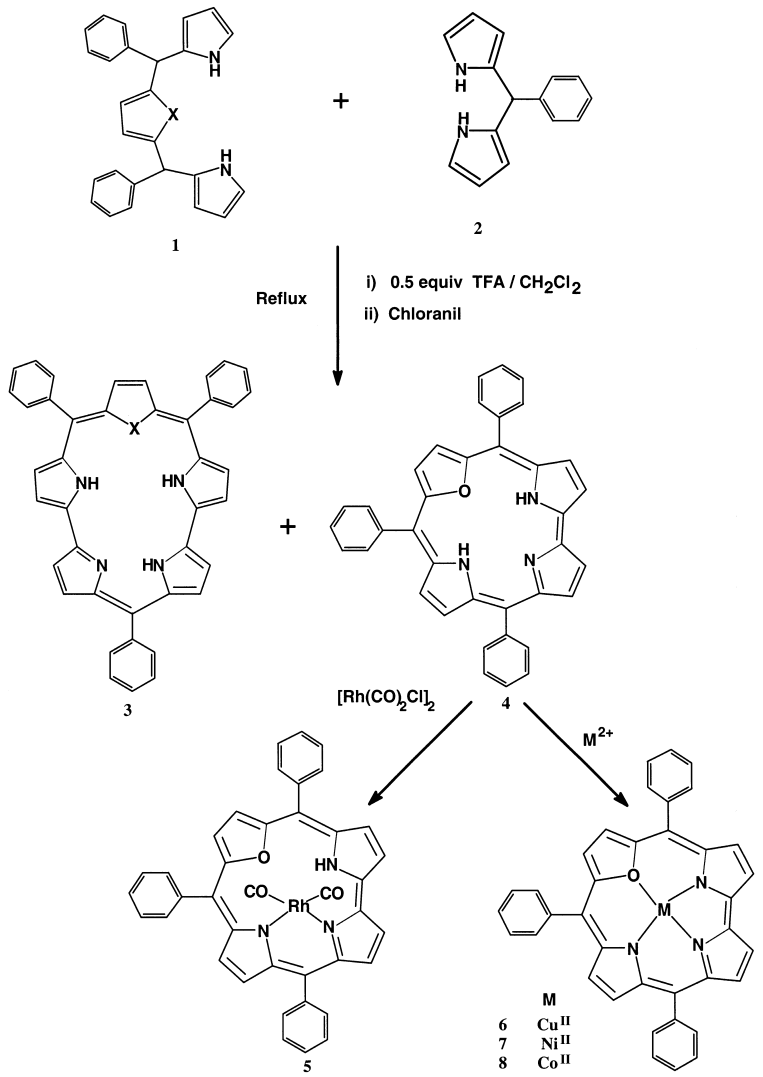

Scheme 1. Synthesis of monooxa corrole and smaragdyrin.

Results and Discussion

Syntheses: The synthesis of normal β-substituted corroles has long been known by metal assisted template reactions.[2] Key factors driving the reaction toward the formation of a contracted corrole ring are the peculiar catalytic activity of the cobalt ion.[8b] In fact, despite the steric hindrance of the β-pyrrole and *meso*-substituents, the corrole can maintain the planar conformation which differs from the related porphyrins where peripheral crowding causes severe deviations from planarity. Eventhough many synthetic methodologies were used to prepare β-substituted corroles, the first *meso*-triphenyl corrole was reported only recently.[8] In this method, the tetraphenyl pophyrinogen was prepared by acid catalyzed condensation of the mono pyrrolic precursor. Further reaction of the porphyrinogen with cobalt gives cobalt(III) corrole. During our early efforts to synthesize monooxa porphyrins[13] by the condensation of 2,5-bis(phenylhydroxymethyl)furan with pyrrole and benzaldehyde in propionic acid medium, we observed the formation of **4** in 2.5% yield along with monooxa porphyrin. Subsequently, in our efforts to synthesize smaragdyrin,[12] which can be termed as an expanded corrole by an unprecedented $\alpha-\alpha$-oxidative coupling of dipyrromethane and tripyrrane (Scheme 1), we were surprised to note the formation of **4** in about 8% yield. Later on, the reaction conditions were modified by varying the acid concentrations as to get the optimum yields of smaragdyrins and corroles. The formation of **4** in this 3+2 reaction is due to the fact that the dipyrromethanes are susceptible to acid catalyzed rearrangements and are known to undergo fragmentation[14] and these products can recombine to give **4** at high concentrations of acid. The metallation of **4** proved straightforward using appropriate metal precursors. However, the ease of metal insertion is generally found to be lower in monooxa corroles in comparison with all normal corroles.

^{1}H-NMR spectroscopy and tautomerism: The ^{1}H-NMR spectrum of **4** was analyzed by considering the effective symmetry of the molecule in solution. The 2D ^{1}H–^{1}H COSY spectrum of **4** is shown in Figure 1 and the assignments are marked. The lower symmetry is reflected in doubling of each pyrrole (dd′) and furan (cc′) resonances thus giving two doublets each for these protons. The bipyrrole protons (bb′) appear as two quartets while the bipyrrole protons (aa′) give two doublets. The appearance of two quartets for bipyrrole protons (bb′) can be attributed to the spatial interaction of the inner -NH proton. These assignments were made on the basis

  0947-6539/00/0614-2555 $ 17.50+.50/0

of correlations observed for various doublets in 2D-COSY and TOCSY experiments.[15] Characteristic sets of cross peaks resulting from the coupling of furan (cc′), pyrrole (dd′), and bipyrrole (aa′, bb′) have been established and are located in the COSY map (Figure 1). In addition, two sets of cross peaks appear for phenyl *ortho*-, *meta*-, and *para* protons; this inequivalence is attributed to the introduction of one furan moiety in the ring. The appearance of cross peaks at $\delta = -1.91$ (inner -NH) and quartet centered around 9.05 and 8.57 in the TOCSY spectrum clearly confirms the through space interaction of inner -NH proton with the bipyrrole protons.

The inner -NH protons are magnetically inequivalent and are expected to show two different resonances. The fact that only one peak is observed down to $-70\,^{\circ}C$ suggests a rapid tautomerism in which these protons are exchanging sites. Of the three possible tautomers I, II, and III, the tautomer I is ruled out from the observation that doublets appear for pyrrole protons (dd′) instead of doublet of doublet. The appearance of doublet of doublet only for one of the bipyrrole protons (pyrrole ring A) suggest localisation of proton on this nitrogen while the other proton is exchanging sites between the pyrrole nitrogens of ring B and C. The X-ray structure (vide infra) shows the predominance of tautomer III.

The protonation of **4** with HF leads to three different -NH signals at $\delta = -2.08$, -2.29, and -4.09, respectively. The pyrrole, furan, and bipyrrole protons experience a slight deshielding effect. These results suggest binding of fluoride ion with three N-H···F hydrogen bonding interaction.[16]

The rhodium complex **5** exhibit significant shielding (up to 0.5 ppm) in one of the bipyrrole protons (aa′) and the pyrrole protons (dd′) (Table 1). This can be accounted in terms of the

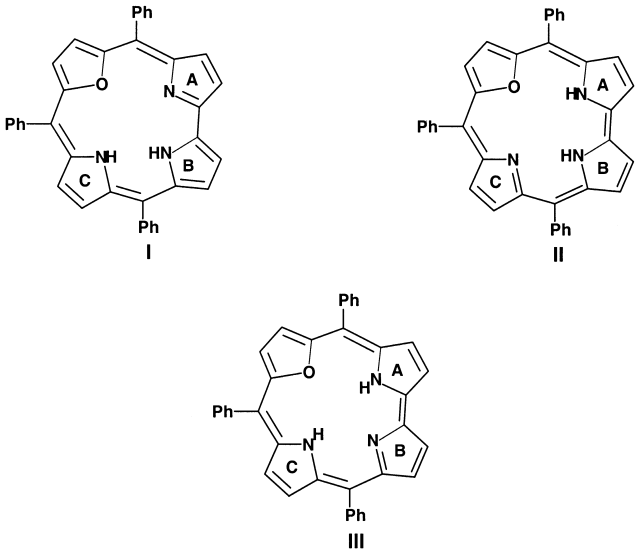

coordination of the metal to the nitrogens containing these protons. Of the two bipyrrole nitrogens, only one of them is coordinated to the metal along with the pyrrole nitrogen. This kind of coordination tilts the two heteroatoms away from the other bipyrrole nitrogen and the furan oxygen which are not coordinated thus causing serious disruption in the electron delocalisation pathway. This observation is in agreement with the X-ray crystal structure of **5** (vide infra). The inner -NH protons attached to the bipyrrole nitrogen which is not coordinated to the metal appear at $\delta = -1.15$ and this is in interaction with bipyrrole protons (bb′) which results in the appearance of doublet of doublets similar to that observed for **4**.

The ^{1}H-NMR spectra of nickel complex **7** does not show any peaks in the negative region thus confirming the coordination of all the heteroatoms to the metal center (Figure 2). Furthermore, the appearance of only doublets for the bipyrrole protons (bb′) confirms the absence of inner -NH proton. All the resonances in the Ni^{II} complex appear within the $\delta = 0-10$ range; this supports the diamagnetic nature of the complex. This is contrast to Ni^{II}-monooxa porphyrin, where the furan and pyrrole protons experience large paramagnetic shifts of up to $\delta = 57$.[17, 18] The X-ray structure (vide infra) of **7** also displays an approximate square planar geometry around the nickel center, in accord with expectation for diamagnetic Ni^{II}.

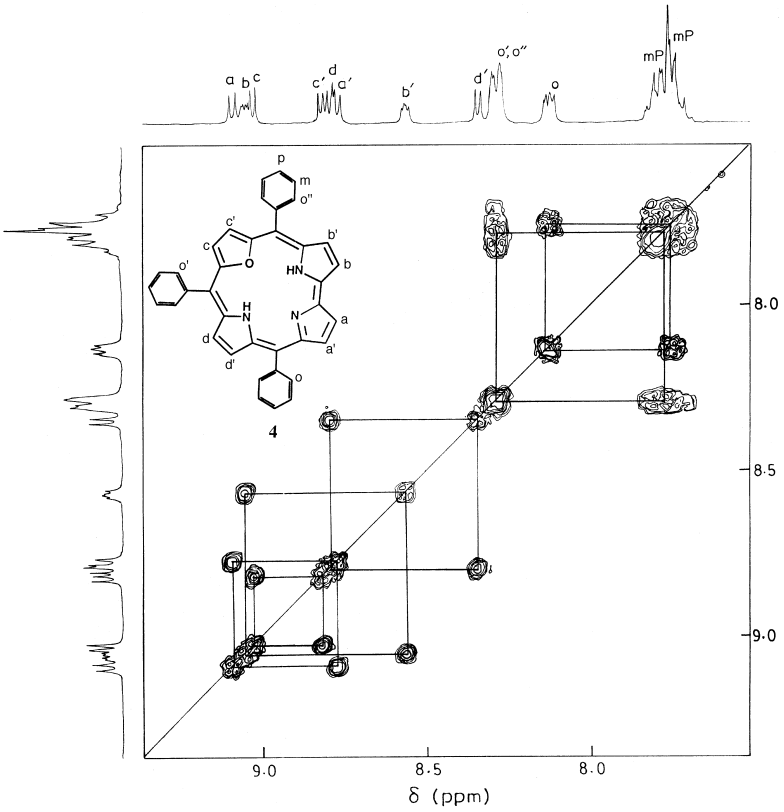

Figure 1. 2D-NMR spectrum (^{1}H–^{1}H COSY) of **4** ($\approx 10^{-4}$ M) in $CDCl_3$ at 25 °C.

0947-6539/00/0614-2556 $ 17.50+.50/0 *Chem. Eur. J.* **2000**, *6*, No. 14

Table 1. ^{1}H-NMR data for monooxa corrole, its protonated form and metallated derivatives.

Corroles	-NH Proton	Phenyl protons				Furan proton	Bipyrrole proton		Pyrrole proton
4	– 1.91 (s)	8.13 (m)	7.73 (m)	8.29 (m)	7.80 (m)	9.03 (d)	9.05 (dd) 1H	8.57 (dd) 1H	8.80 (d)
	1H	2H	3H	4H	6H	1H, $J = 4.2$ Hz	$J_{AB} = 4.2$ Hz	$J_{AB} = 5.4$ Hz	1H, $J = 4.8$ Hz
						8.82 (d)	$^4J_{H,H} = 2.4$ Hz	$^4J_{H,H} = 2.6$ Hz	8.35 (d)
						1H, $J = 4.2$ Hz	9.09 (d) 1H	8.78 (d) 1H	1H, $J = 4.5$ Hz
							$J = 5.1$ Hz	$J = 5.1$ Hz	
5	– 1.15 (s)	8.11 (m)	7.75 (m)	8.18 (m)	7.75 (m)	9.08 (d)	9.02 (dd) 1H	8.62 (dd) 1H	8.32 (d)
	1H	2H	3H	4H	6H	1H, $J = 5.0$ Hz	$J_{AB} = 4.0$ Hz	$J_{AB} = 5.2$ Hz	1H, $J = 4.0$ Hz
						8.90 (d)	$^4J_{H,H} = 2.1$ Hz	$^4J_{H,H} = 2.4$ Hz	7.87 (d)
						1H, $J = 5.0$ Hz	8.64 (d) 1H	8.18 (d) 1H	1H, $J = 4.5$ Hz
							$J = 4.0$ Hz	$J = 4.0$ Hz	
7	–	8.05 (m)	7.70 (m)	8.16 (m)	7.74 (m)	8.90 (d)	9.05 (d) 1H	8.74 (d) 1H	8.79 (d) 1H
		2H	3H	4H	6H	1H, $J = 4.6$ Hz	$J = 5.6$ Hz	$J = 5.6$ Hz	$J = 4.6$ Hz
						8.60 (d)	8.97 (d) 1H	8.49 (d) 1H	8.39 (d)
						1H, $J = 4.6$ Hz	$J = 4.4$ Hz	$J = 4.4$ Hz	1H, $J = 4.9$ Hz
4·HF	– 2.08 (s), 1H	8.40 (m), 2H; 8.31 (m), 2H; 8.16 (m), 2H				9.32 (d)	9.06 (d) 1H	8.50 (d) 1H	8.92 (d), 1H
	– 2.29 (s), 1H					1H, $J = 5.0$ Hz			
	– 4.09 (s), 1H	7.83 (m), 3H; 7.77 (m), 3H; 7.73 (m), 3H				9.02 (d)	8.98 (d) 1H	8.51 (d) 1H	8.53 (d), 1H
						1H, $J = 4.9$ Hz			

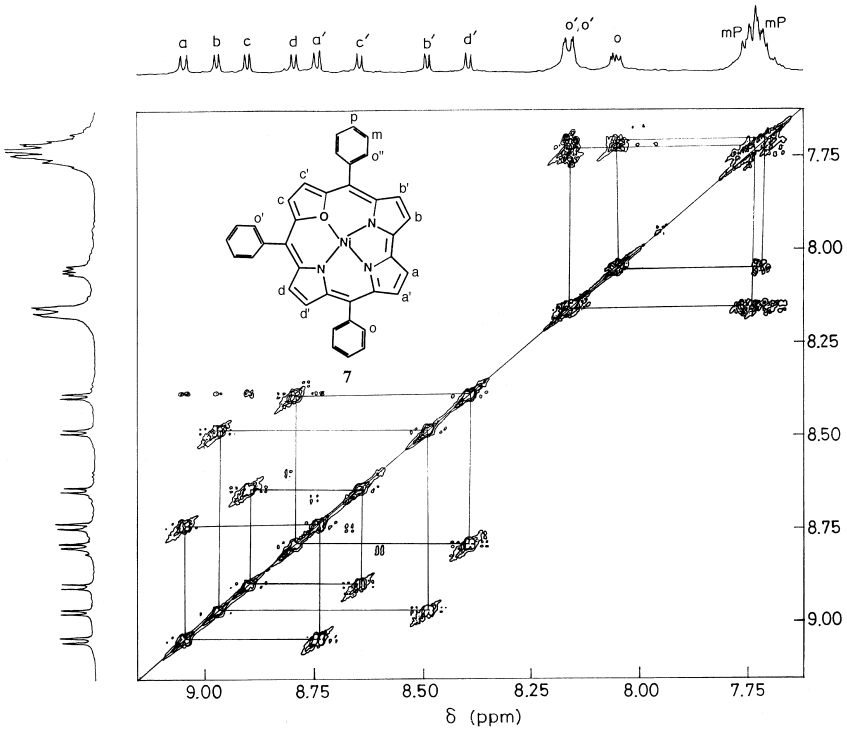

Figure 2. 2D-NMR spectrum (^{1}H–^{1}H COSY) of **7** ($\approx 10^{-4}$ M) in $CDCl_3$ at 25 °C.

Spectral characterization: The electronic spectra of **4** is shown in Figure 3. A Soret type intense band (411 nm) and four Q-type bands (490–640 nm) are obvious in the visible region. The observed hypsochromic shift of these bands when compared to 5,10,15-triphenylcorrole is due to the replacement of one nitrogen by oxygen in the central core. This observation is similar to changes observed on going from tetraphenylporphyrin (H_2TPP) to monooxa-tetraphenylporphyrin (OTPPH).[13] Unlike the normal corrole, there is no variation in the pattern of spectrum obtained for **4** in a basic solvent such as DMF; this suggests that the monooxa corrole is less acidic relative to normal corrole.[11] On protonation with TFA, the Soret band is split, which is due to the lowering of symmetry in solution. The spectroscopic properties suggest that **4** is aromatic and is consistent with the presence of $[4n+2]$ π-electrons. The chemical shifts of the pyrrole, furan and inner -NH resonances in ^{1}H-NMR spectra further support the aromatic nature of **4**.

Corrole **4** surprisingly show very strong emission with a quantum yield of 0.88 relative to H_2TPP (Figure 3 inset). The emission maxima is strongly blue shifted relative to the corresponding porphyrin. Protonation of **4** leads to red shift of emission band and the quantum yield (0.23) for the protonated derivative is also higher than the corresponding porphyrins. Lifetime measurements indicate a lifetime of 6.04 ns for **4** and the radiative and nonradiative rate constants estimated from the relations $k_r = \phi_f/\tau$ and $k_{nr} = 1/\tau - k_r$ (k_r = radiative rate constant, k_{nr} = nonradiative rate constant, ϕ_f = fluorescence quantum yield, τ = lifetime) are 1.45×10^8 s^{-1} and 0.2×10^8 s^{-1}. These values are higher and lower relative to H_2TPP ($k_r = 0.12 \times 10^8$ s^{-1}, $k_{nr} = 0.99 \times 10^8$ s^{-1}) consistent with the high quantum yield of **4**. It is surprising that even metal derivatives **5**, **6**, **7**, and **8** emit fluorescence.

The absorption spectra for the metallated derivatives of **4** shown in Figure 4 reveal that the characteristic Soret type and Q-type bands in the region 400–700 nm is retained on metallation. The spectra for **6** and **8** exhibit a broad Soret band while **5** and **7** show split Soret bands revealing their lower symmetry in solution. The effect of core modification and the *meso* substitution are reflected in the significant red shifts of these absorption bands in **5**, **6**, **7**, and **8** relative to the

  0947-6539/00/0614-2557 $ 17.50+.50/0

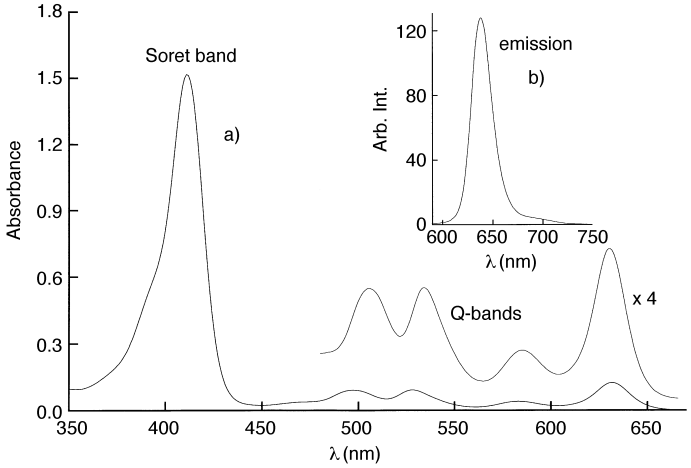

Figure 3. a) UV/Vis spectra for **4** (5.31×10^{-6} M) in dichloromethane, b) emission spectra (inset) for **4** (5.31×10^{-6} M) in dichloromethane. $\lambda_{ex} =$ 411 nm.

corresponding metal derivatives of β-substituted corroles reported by Vogel and co-workers.[19] The ε-values of all the metallated derivatives in both the cases are about 50% smaller than those of corresponding free base derivatives suggesting a decreased π-electron conjugation upon metal insertion.

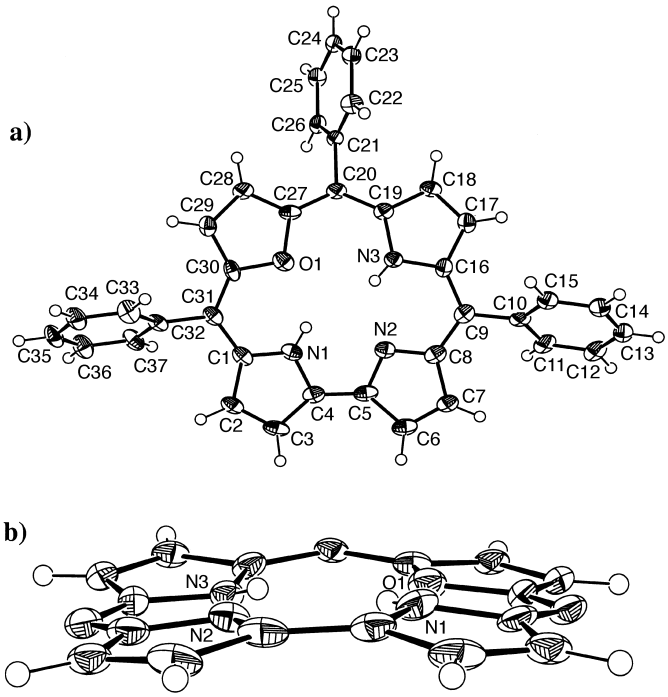

Figure 5. ORTEP diagram for **4** a) top: plane view; b) bottom: side view (phenyl rings are omitted for clarity).

Crystallographic characterization: The structure of freebase **4** was confirmed by single crystal X-ray crystallography (Figure 5). The structural characterization of freebase β-substituted corrole was reported by Hodgkin and co-workers[20] in the early seventies. It was observed that the geometry of the 8,12-diethyl-2,3,7,13,17,18-hexamethyl corrole is nonplanar due to the short N–N contacts brought by the reduction in one *meso*-carbon atom. Also, here three inner hydrogen atoms are statistically distributed among the four nitogen atoms.

The structure reported for the monooxa corrole turned out to be the first characterisation of core modified mesoaryl corrole. The bond lengths and the bond angles compare well with the reported β-substituted corrole[20]. The C_α–C_β bond lengths are longer than the C_β–C_β distances showing the evidence for aromatic nature. [C_α–C_β: C_1–$C_2 = 1.423(6)$ Å; C_3–$C_4 = 1.410(6)$ Å; C_{27}–$C_{28} = 1.407(6)$ Å; C_{29}–$C_{30} = 1.418(6)$ Å; C_β–C_β: C_2–$C_3 = 1.381(6)$ Å; C_{28}–$C_{29} = 1.377(6)$ Å]. The corrole ring exhibits almost planar structure with only small deviations from the planarity varying from

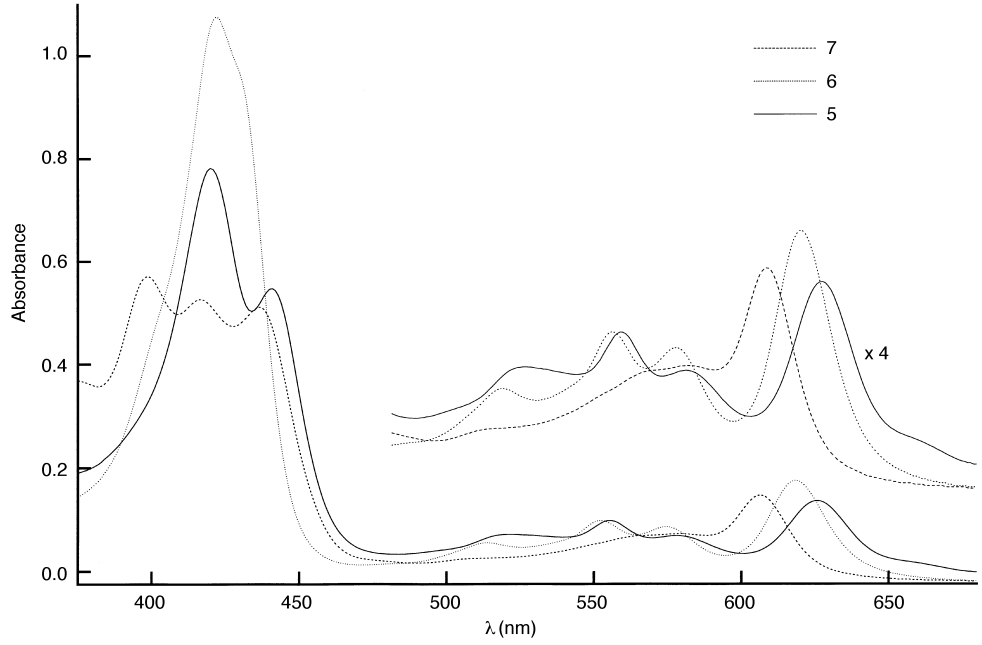

Figure 4. Overlay UV/Vis spectra of **5** (6.80×10^{-6} M), **6** (8.13×10^{-6} M), and **7** (6.84×10^{-6} M) in dichloromethane.

0947-6539/00/0614-2558 $ 17.50+.50/0 *Chem. Eur. J.* **2000**, *6*, No. 14

5.48° to 7.74°. This is quite different from a recent report on 5,10,15-tri(pentafluorophenyl)corrole reported by Gross et al.[10b] where significant deviations of the pyrrole rings are observed. Specifically, the pyrrole rings are turned slightly either up or down with twist angles between the rings increase in moving clockwise varying from 4.4° to 19.5°. This is due to the increased steric hindrance between the three inner pyrrole protons. However, in the present case, since one of the pyrrole ring is replaced by furan ring, there are only two pyrrole hydrogens decreasing the strain on the macrocycle. Unlike in the case of β-substituted corrole, the inner hydrogen atoms in **4** are clearly identified in the electron density maps on the N1 and N3 nitrogen atoms. The nonbonded N–N distances are almost comparable with that of β-substituted corrole. This is due to an almost similar size of oxygen and nitrogen atoms [β-substituted corrole: N1–N2 = 2.53 Å, N2–N3 = 2.66 Å, N3–N4 = 2.89 Å, N4–N1 = 2.72 Å; **4**: N1–N2 = 2.55 Å, N2–N3 = 2.61 Å, N3–O1 = 2.99 Å, O1–N1 = 2.63 Å].

Another important feature of the structure is the presence of strong $\pi-\pi$ interactions between the macrocycles with average plane to plane separations of 3.613 Å; this leads to a spectacular columnar structure.[12] Even in case of β-substituted corrole,[20] the assymmetric units pack as parallel discs in stacks thus assuming a "herring bone" structure with nonbonded aliphatic contacts aiding in molecular positioning. The lengths of these contacts (3.53 – 4.25 Å) which is more or less similar to **4**, suggest that the stacks are quite closely packed.

The crystal structure of **5** is shown in the Figure 6. According to the X-ray structure, the Rh^I ion is located above the corrole plane and the geometry around the metal center is close to square planar (C39-Rh1-N2 94.1(2)°, C38-Rh1-N3 94.4(2)°). One imino and one amino nitrogen of the macrocycle is coordinated to the Rh^I ion and the other two coordination sites are occupied by carbonyl ligands. This is consistent with the earlier observation of requirement of one amino and one imino nitrogen for the stabilization of Rh^I ion in the macrocyclic environment.[21a] Eventhough monooxa corrole has one imino (N2) nitrogen which is between the two amino (N1 and N3) nitrogens, the coordination of Rh^I takes place only at N2 and N3 nitrogen atoms. This is probably due to the fact that this type of coordination will avoid strain in the molecule which otherwise will happen due to the direct C4–C5 link. Also there are strong intramolecular hydrogen bonding between the N1-H···O1 (2.63 Å, 122.35°) and N1-H···N2 (2.67 Å, 106.82°).

Due to the out of plane coordination of Rh^I ion, the pyrrole rings containing N2 and N3 are twisted above the mean corrole plane by an angle of 23.51° and 19.69°, respectively. The angle between the plane containing the Rh^I with its coordinated atoms and the mean corrole plane is 62.64°. The macrocycle is nonplanar and this is reflected in the increase of the nonbonded heteroatom distances relative to freebase monooxa corrole. [O1–N3: 3.068 Å, O1–N1: 2.631 Å, N1–N2: 2.668 Å, N2–N3: 2.654 Å]. A comparison of Rh–N and Rh–C distances observed for **5** with that of other Rh^I complex of β-substituted corroles[21b] (Table 2) suggest that the substitution of methyl groups on the pyrrole does not alter these distances significantly.

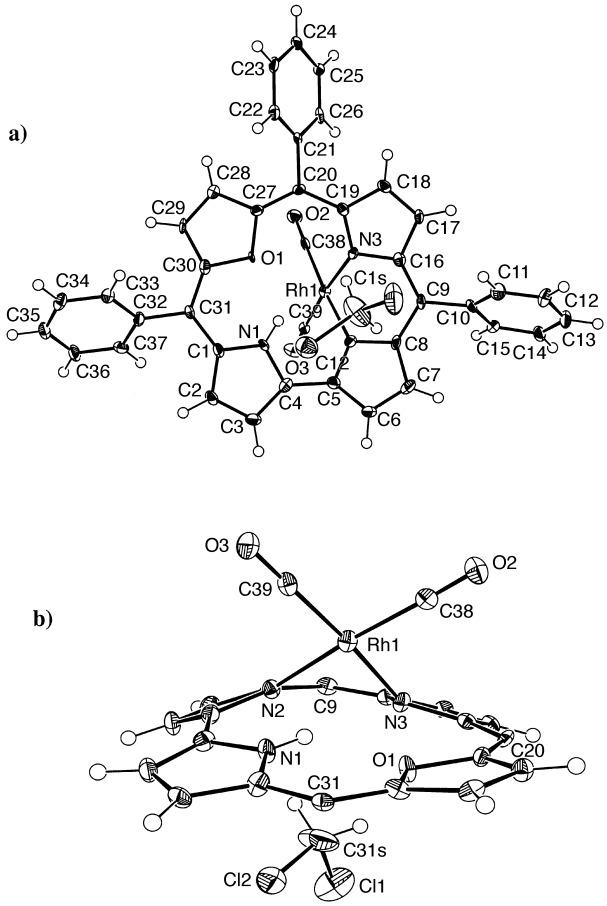

Figure 6. ORTEP diagram for **5** a) top: plane view; b) bottom: side view (phenyl rings are omitted for clarity).

Table 2. A comparison of selected interatomic distances for Rh^I complexes.

Rhodium complexes	Rh–N2 (Å)	Rh–N3 (Å)	Rh–C38 (Å)	Rh–C39 (Å)	Ref.
N-21-methyl corrole	2.059(9)	2.069(9)	1.854(14)	1.849(13)	[22]
N-22-methyl corrole	2.048(4)	2.062(4)	1.843(6)	1.850(6)	[22]
5	2.052(4)	2.061(4)	1.860(5)	1.851(6)	present work

The incorporation of nickel to the corrole core flattens the macrocycle almost to a planar structure as seen from the Figure 7. There are two ionisable protons and hence the metal is expected to be in the oxidation state of +2 unlike in the case of β-substituted corroles.[19] The Ni^{II} atom acquires a distorted square planar conformation which is due to the direct C4–C5 link[N1-Ni-N2: 82.76 (12)°]. The Ni atom lies above the mean plane of the macrocycle by only 0.008 Å. The deviation of the heterocyclic ring from the mean plane of the corrole ring are O1 5.90, N1 4.95, N2 6.47, N3 8.00° and for the free base they are 5.48, 7.40, 6.09, 7.74°, respectively. A comparison of Ni–N and Ni–O distances (Table 3) shows that they are shorter when compared with the corresponding distances of porphyrins[17] thus reflecting reduced core size in oxa corroles. As expected, the two shortest Ni–N bonds are those involving nitrogens adjacent to C_α–C_α link, and this is typically observed

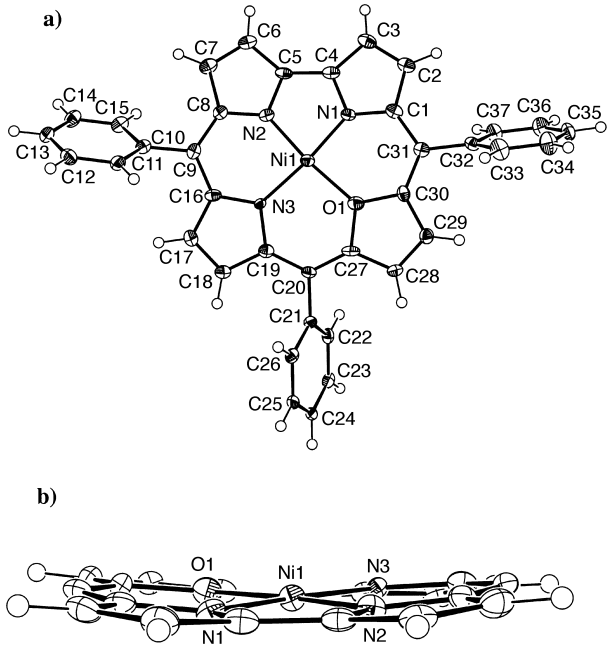

Figure 7. ORTEP diagram for **7** a) top: plane view; b) bottom: side view (phenyl rings are omitted for clarity).

Table 3. A comparison of selected interatomic distances for Ni^{II} complexes.

Nickel complexes	Ni–N1 (Å)	Ni–N2 (Å)	Ni–N3 (Å)	Ni–X, X = N,O,S (Å)	Ref.
NiCORR	1.836(3)	1.829(3)	1.859(3)	1.858(3)	
NiOTPP	2.004(6)	1.955(5)	2.063(5)	2.185(5)	[19]
NiSTPP	2.095(3)	1.963(4)	2.084(3)	2.296(1)	[17a]
7	1.832(3)	1.827(3)	1.887(3)	1.906(2)	[17b]

for metallo corroles.[8b, 19] The incorporation of the metal ion decreases the N1–N2 (2.419 Å) and N3–O1 (2.815 Å) nonbonding distances and increases the N1–O1 (2.655 Å) and N2–N3 (2.647 Å) nonbonding distances.

ESR Spectroscopy: All normal corroles have three ionisable NH protons and hence are expected to stabilize trivalent metal cations. Recent studies from Vogel and co-workers[19] has settled the previous controversy regarding the oxidation states of copper and nickel corroles. Specifically they have shown that the nickel corrole exist as nickel(II) complex and the unpaired electron is centered on one of the *meso* carbons while for the copper complex there exists an equilibrium between copper(III) corrole and copper(II) corrole with the unpaired electron centered on the *meso* carbon. This equilibrium is temperature dependent, higher temperature favoring the copper(II) corrole with unpaired electron while the lower temperature favoring the copper(III) corrole formulation. In the complexes of monooxa corrole there are only two ionisable NHs and authentic Cu^{II}, Ni^{II}, and Co^{II} complexes are expected. The Cu^{II} and Co^{II} complexes are amenable for ESR studies and the spectra of **6** in Figure 8 shows a resolved spectra in which two of the four copper parallel lines are seen and the third line is overlapped by the much stronger perpendicular lines, while the fourth line is invariably completely overlapped. Furthermore, the superhyperfine splittings from the coordinated nitrogens are also observed,

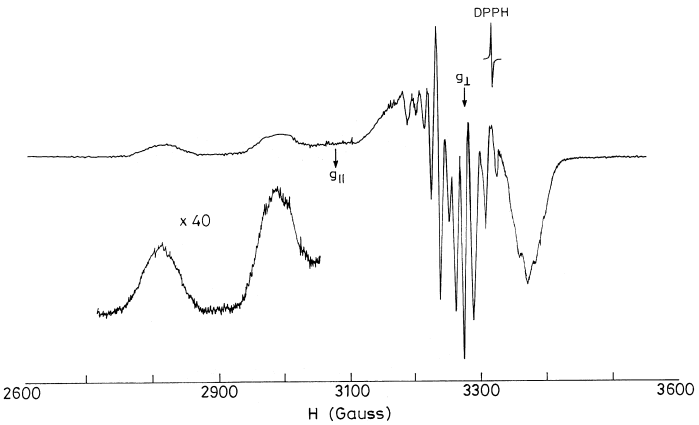

Figure 8. EPR spectrum of **6** in toluene/dichloromethane 1:1 at 77 K. The concentrations used were $\approx 10^{-3}$ M; dpph = diphenylpicrylhydrazyl.

confirming the presence of electron delocalisation into the ligand orbitals. A comparison of the ESR parameters (Table 4) reveals that there is a slight decrease in $g_{\|}$ and $g_{\perp}$ values, but a significant reduction in $A_{\|}^{Cu}$ and $A_{\perp}^{Cu}$ values. The hyperfine coupling constants of copper are quite sensitive to distortions from square planar geometry. It has been shown that, for a tetrahedral geometry, $A_{\|}^{Cu}$ lies in the range 100–140 (10^{-4}) cm^{-1} and $A_{\perp}^{Cu}$ in the range 50–07 (10^{-4}) cm^{-1}.[22] The observed value for **6** suggests a moderate deviation from the square planar geometry. Also, if copper is displaced above the plane of the ring then direct mixing of 4s orbital to the ground state of Cu^{II} caused by symmetry lowering is also

Table 4. A comparison of EPR parameters for Cu^{II} and Co^{II} complexes.

Metal complex	$g_{\|}$	$g_{\perp}$	$A_{\|}^{Cu}$ 10^{-4} cm^{-1}	$A_{\perp}^{Cu}$ 10^{-4} cm^{-1}	Ref.
CuTPP[a]	2.185	2.045	202.0	33.0	[25]
CuOTPP[b]	2.249	2.036	118.0	25.7	[18]
6[c]	2.158	2.029	165.0	25.6	present work
CoTPP[d]	1.970	2.800	141.0	210.0	[25]
α-CoPc[e]	2.007	2.422	116.0	66.0	[25, 26]
8	1.930	2.240	78.0	56.0	present work

[a] Copper tetraphenylporphyrin. [b] Copper 21-oxa tetraphenylporphyrin. [c] $A_{\perp}^{N}$ for **6** = 12.8 cm^{-1}. [d] Cobalt tetraphenylporphyrin. [e] α-Cobalt phthalocyanine.

reponsible for the decrease in $A_{\|}^{Cu}$ values.[23] The inplane σ covalency parameter α^2_{Cu} is related to $A_{\|}$, $g_{\|}$, $g_{\perp}$ according to the equation $\alpha^2_{Cu} = A_{\|}/0.036 + (g_{\|} - 2.0023) + 3/7(g_{\perp} - 2.0023) + 0.04$.[24] This value accounts for the fraction of unpaired electron density on the copper(II) ion. A value of 0.67 observed for **6** indicates more covalent character of Cu–N bond relative to CuTPP ($\alpha^2_{cu} = 0.82$).

Cobalt complex of monooxa corrole was prepared and the ESR spectrum at 77 K along with the room temperature spectrum are shown in Figure 9. In general, the EPR spectra of cobalt(II) complexes are very sensitive to the presence of dissolved oxygen in the solvent as well as to the change in the geometry. The presence of oxygen broadens the spectrum with the decrease in cobalt hyperfine values due to the formation of $Co-O_2$ adduct.[25] In the present study, the EPR

0947-6539/00/0614-2560 $ 17.50+.50/0 *Chem. Eur. J.* **2000**, *6*, No. 14

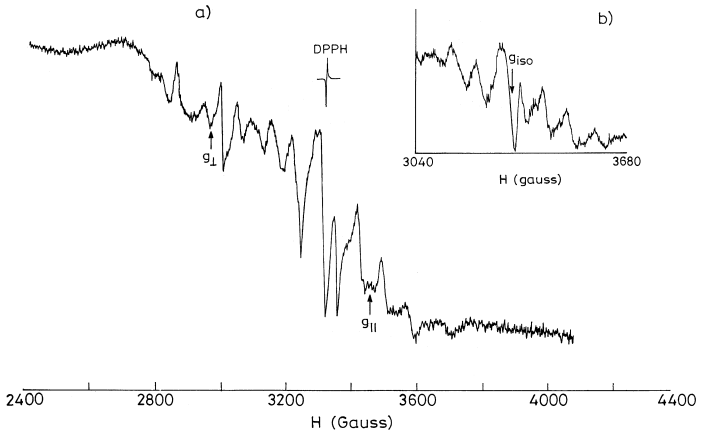

Figure 9. EPR spectrum of **8** in toluene/dichloromethane 1:1; a) at 77 K; b) at room temperature (inset). The concentrations used were $\approx 10^{-3}$ M.

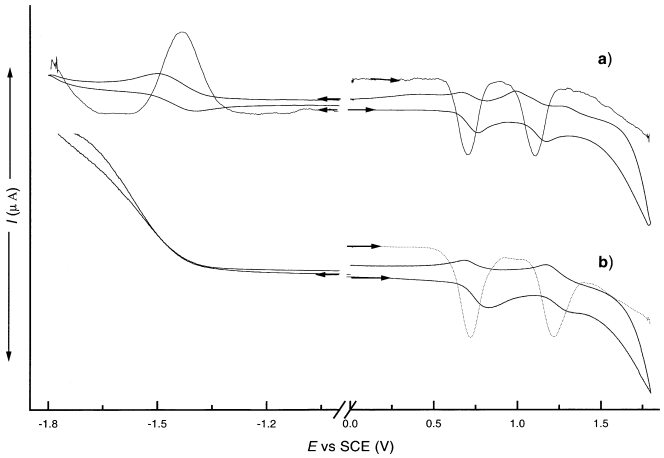

Figure 10. Cyclic voltammograms and differential pulse voltammograms of a) **4** and b) **7** in dichloromethane recorded at 50 mV s^{-1} scan speed. 0.1 M $TBAPF_6$ was used as the supporting electrolyte.

spectra were recorded by preparing the sample under freeze–thaw technique to eliminate the dissolved oxygen. From Table 4, it can be seen that **8** is uniquely different from CoTPP, but similar to α-Co phthalocyanine[26] having a unusually smaller A tensor, $g_{\parallel}$ and $g_{\perp}$ values.

Unlike the copper complexes the study of Co (d^7) systems by ESR offers the possibility for a close look at the a_1 orbital. It has been shown that the ESR parameters, g and A depends strongly on the relative levels of a_1 and e orbitals.[25] The decrease in g and A values can be qualitatively interpreted as resulting from the gradual increase of the orbital energy of a_1 with respect to that of e.[25] This is in contrast to that observed for cobalt(II) corrole anion[27] where the unpaired electron is believed to be in $d_{x^2-y^2}$ orbital.

Electrochemical studies: Electrochemical data of monooxa corrole along with various other porphyrins are listed in Table 5. Typical cyclic voltammograms overlayed with differential pulse voltammograms of free base and nickel corrole

Table 5. Luminescent and electrochemical data for various porphyrins and corrole.

Porphyrins	$E_{1/2}$ red (I) [V]	$E_{1/2}$ ox (I) [V]	Δ_{redox} Δ_{redox}	ϕ[a] V	$E_{0\text{-}0}$(p–p*) [eV]	E^0 (*p/p-) [V]	E^0 (p+/p*) [V]
4	–1.46	0.72	2.18	0.880	1.94	0.48	–1.22
H_2TPP	–1.23	1.03	2.26	0.110	1.90	0.67	–0.87
OTPPH	–1.20	–	–	0.075	1.82	0.62	–
STPPH[b]	–1.06	1.04	2.00	0.017	1.82	0.76	–0.74

[a] Relative to H_2TPP. [b] 21-Thia tetraphenylporphyrin.

are shown in Figure 10. Corrole **4** gives one quasi reversible ring reduction ($\Delta E_p = 98$ mV) and two quasi reversible ring oxidations ($\Delta E_p = 103$ mV and 207 mV, respectively). A comparison of the oxidation potentials of **4** relative to the corresponding porphyrins suggests easier oxidation to an extent of 310 mV. On the other hand, the reduction of **4** is harder relative to all other porphyrins by about 230 mV. The excited state reduction and oxidation potentials[28] estimated from the emission and ground state reduction and oxidation potentials indicate that they are better electron acceptors and poor electron donors in the excited state.

The metal derivatives **6** and **7**, surprisingly did not show the expected metal reduction peaks. Generally it is known in literature that the metal derivatives of β-substituted corroles show metal centered reductions.[19] The failure to see any metal centered reductions in the complexes of *meso*-aryl corroles indicates that the LUMO in the metal complexes are high in energy and are not accessible in the solvent window of dichloromethane.

Conclusion

Synthesis of the first core modified *meso*-aryl corrole directly in its free-base form has been achieved by an $\alpha-\alpha$ coupling reaction of easily available precursors. With the availibility of this modified corrole, it is possible to synthesize authentic divalent metal complexes. The different modes of binding of Ni^{II} and Rh^{I} to monooxa corrole is interesting from the structural point of view. We hope that with the availability of facile synthetic methods from three different laboratories for the preparation of *meso*-aryl corroles and their metal derivatives will attract renewed impetus and allow a development of their fascinating chemistry. The high quantum yield observed for free-base monooxa corrole reported here opens up the possibility for its potential use as an efficient flourescent sensors. Efforts are currently under way in this direction.

Experimental Section

Instrumentation: Electronic spectra were recorded on a Perkin–Elmer Lamda 20 UV/Vis spectrophotometer. Emission spectra were obtained from Perkin–Elmer LS 50 B luminescence spectroflourimeter interfaced to the computer. The data analysis was done using the fluorescence data manager program. Chemical analyses (C, H, N) were done on a Heraeus Carlo Elba 1108 elemental analyser. Proton NMR spectra were obtained either on a 500 MHz Bruker spectrometer or on a 400 MHz JEOL spectrometer in $CDCl_3$. Chemical shifts are expressed in parts per million relative to residual $CHCl_3$ ($\delta = 7.258$). FAB-MS spectra were obtained on a JEOL SX-120/DA6000 spectrometer. ESR measurements were done on a varian E-109 X-band spectrometer at room temperature and liquid

nitrogen temperature. Cyclic voltammetric studies were done on a EG/G PAR model 273A polorographic analysis interfaced to the computer. A three electrode system consisting of a platinum working electrode, a platinum mesh counter electrode and a commercially available saturated calomel electrode (SCE) as the reference electrode were used. This reference electrode was separated from the bulk of solution by a fritted glass bridge filled with the solvent/supporting electrolyte mixture. Half-wave potentials were measured as the average of the cathodic and anodic peak potentials. Lifetime measurements were done using time correlated single photon counting technique using an IBH 5000 nanosecond fluorescence spectrometer consisting of a nitrogen damp operating at 40 kHz with an maximum at 337 nm. Hamamatsu C4878 series is a water-cooled high performance thermoelectric cooler for microchannel plate incorporated photomultipliers (MCP PMT). Florescence decay analysis was done by IBH software which contains the reconvolution fitting programs, graphics, statistical and utility programs.

X-ray structure determinations: X-ray quality crystals for all compounds were grown using the solvent mixture given in the Table 6 by the diffusion method. The crystals were removed from the Schlenk tube under a steam of N_2 and immediately covered with a layer of viscous hydrocarbon oil (Paratone N, Exxon).[29] A suitable crystal was selected with a microscope, attached to a glass fiber, and immediately placed in the low temperature, attached to a glass fiber, and immediately placed in the low temperature N_2 stream of the diffractometer. Data sets for all the compounds were collected using a Siemens SMART system, complete with three-circle goniometer and CCD detector operating at $-54\,^{\circ}C$. The data sets were collected at 98(1), 94(5) and 89(7) K with a home-made low temperature device, by employing graphite monochromated $Mo_{K\alpha}$ radiation ($\lambda =$ 0.71073 Å). The data collections nominally covered a hemisphere of reciprocal space utilizing a combination of three sets of exposures, each with a different ϕ angle, and each exposure covering 0.3° in ω. Crystal decay was monitored by repeating the initial frames at the end of the data collection and analyzing the duplicate reflections. In all cases, no decay was observed. An absorption correction was applied utilizing the program SADABS.[30] The crystal structures of all composunds were sovled by direct methods, as included in SHELX program package. Missing atoms were located in subsequent difference Fourier maps and included in the refinement. The structures were refined by full-matrix least-squares refinement on F^2 (SHELX-93).[31, 32] Hydrogen atoms at nitrogens for **4** were located in difference fourier cycles and included in the refinement. All other hydrogen atoms were placed geometrically and refined using a riding model. The hydrogen atoms in all compounds were refined with Uiso constrained at 1.2 times Ueq of the carrier C atom. Scattering factors were those provided by the SHELX program. All non-hydrogen atoms were refined anisotropically. Further details about the refinements is outlined in the supplementary material.

Crystallographic data (excluding structure factors) for the structures of **5** and **7** reported in this paper have been deposited with the Cambridge Crystallographic Data Centre as supplementary publication no. CCDC-135916 and CCDC-135917. Copies of the data can be obtained free of charge on application to CCDC, 12 Union Road, Cambridge CB2 1EZ, UK (fax: (+44) 1223-336-033; e-mail: deposit@ccdc.cam.ac.uk). Crystallographic parameters for compounds **4**, **5** and **7** are summarised in the Table 6. For compound **4**, see ref. [12].

Chemicals: All NMR solvents were used as received. Solvents like dichloromethane, tetrahydrofuran (THF), dimethylformamide (DMF) and *n*-hexane were purified and distilled by standard procedures. Tetra-*n*-butyl ammonium hexaflourophosphate from Fluka was used as the supporting electrolyte for cyclic voltammetric studies. 2,5-Bis(phenyl hydroxy methyl)furan, dipyrromethane (**2**), and 16-oxatripyrrane (**3**) were prepared according to the published procedure[13] and stored under inert atmosphere at $-10\,^{\circ}C$.

Syntheses

5,10,15-Triphenyl-21-oxacorrole(4): This can be prepared by two methods.

a) 2,5-Bis(phenyl hydroxy methyl)furan (0.22 g, 0.78 mmol), benzaldehyde (0.16 mL, 1.56 mmol), and pyrrole (0.16 mL, 12.36 mmol) were dissolved in freshly distilled propionic acid (75 mL). The mixture was refluxed for 1 h and left at room temperature for 24 h. The solvent was removed under reduced pressure. The crude product was thoroughly washed with hot water and was dissolved in chloroform and washed with 25% ammonia (50 mL) followed by water and dried over anhydrous Na_2SO_4. The solvent was removed and the crude product was purified by column chromatography over basic alumina column with petroleum ether and dichloromethane. A pink band eluted with petroleum ether/dichloromethane 5:1 gave a purple solid identified as **4** (10 mg, 2.5%). UV/Vis (CH_2Cl_2): λ_{max} ($\varepsilon \times 10^{-4}$) = 411 (27.0), 497 (1.6), 528 (1.6), 583 (0.7), 632 nm (2.1 $mol^{-1}dm^3cm^{-1}$); UV/Vis (CH_2Cl_2/HCl): λ_{max} ($\varepsilon \times 10^{-4}$) = 412 (24.3), 431sh (13.7), 523 (3.2), 583 (0.3), 635 nm (5.4 $mol^{-1}dm^3cm^{-1}$); emission (CH_2Cl_2): $\lambda = 640$ nm; emission (CH_2Cl_2/HCl): $\lambda = 652$ nm; FAB-MS: *m*/*z*: 528 $[M]^+$; anal. calcd for $C_{37}H_{25}N_3O$: C 84.23, H 4.78, N 7.96. found: C 84.27, H 4.75, N 7.99.

Table 6. Crystallographic data for monooxa corrole, rhodium oxacorrole, and nickel oxacorrole.

Crystallographic data	**4**	**5**	**7**
solvent for crystallisation	CH_2Cl_2/*n*-hexane	CH_2Cl_2/MeOH	CH_2Cl_2/*n*-heptane
empirical formula	$C_{37}H_{25}N_3O$	$C_{40}H_{26}Cl_2N_3O_3Rh$	$C_{37}H_{23}N_3ONi$
T [K]	98(2)	94(2)	89(2)
crystal system	orthorhombic	triclinic	orthorhombic
space group	$P2_12_12_1$	$P\bar{1}$	$P2_12_12_1$
V [Å^3]	2654.56(6)	1624.8(2)	2635.5(4)
a [Å]	6.4881(10)	9.5012(8)	6.4079(6)
b [Å]	18.0075(2)	13.3702(11)	18.2288(16)
c [Å]	22.7207(3)	13.7434(12)	22.562(2)
α [°]	90	92.351(2)	90
β[°]	90	107.662(2)	90
χ [°]	90	100.851(2)	90
Z	4	2	4
ρ_{calcd} [mg m^{-3}]	1.320	1.575	1.473
refl. measured/	17980	11194	17996
unique	4659	7599	6411
R(int)	0.1272	0.0499	0.0716
F(000)	1104	780	1208
limiting	$-7 \le h \le 7$, $-18 \le k \le 21$,	$-5 \le h \le 12$, $-17 \le k \le 16$,	$-8 \le h \le 8$, $-17 \le k \le 23$,
indices	$-27 \le l \le 26$	$-18 \le l \le 16$	$-29 \le l \le 30$
GoF (F^2)	0.975	0.968	1.014
final R indices [$I > 2\sigma(I)$]	$R_1 = 0.0762$	$R_1 = 0.0643$	$R_1 = 0.0511$
	$wR_2 = 0.1721$	$wR_2 = 0.1243$	$wR_2 = 0.0937$
R indices (all data)	$R_1 = 0.1094$	$R_1 = 0.1270$	$R_1 = 0.0862$
	$wR_2 = 0.1870$	$wR_2 = 0.1436$	$wR_2 = 0.1039$

0947-6539/00/0614-2562 $ 17.50+.50/0 *Chem. Eur. J.* **2000**, *6*, No. 14

b) 16-Oxatripyrrane (**1**, 0.51 g, 1.36 mmol) and dipyrromethane **2** (0.29 g, 1.36 mmol) were dissolved in dry dichloromethane (400 mL) and stirred under nitrogen atmosphere for 5 min. TFA (0.05 mL, 0.68 mmol) was added and the stirring continued for further 90 min. Chloranil (1 g, 4.068 mmol) was added and the reaction mixture was exposed to air and refluxed for further 90 min. The solvent was evaporated in vacuo. The residue was purified by chromatography on a basic alumina column. The pink fraction which eluted with petroleum ether/dichloromethane 5:1 was identified as monooxa corrole **4** (60 mg, 8.3 %) which decomposes above 270 °C. The second green band eluted with dichloromethane gave **3** (160 mg, 20 %), which decomposes above 250 °C. ^{1}H NMR (300 MHz, $CDCl_3$, 25 °C, TMS): δ = 7.83 (m, 9H), 8.21 (m, 4H), 8.38 (m, 2H), 8.42 (d, J = 4.2 Hz, 2H), 8.74 (s, 2H), 8.95 (d, J = 4.2 Hz, 2H), 9.36 (d, J = 4.2 Hz, 2H), 9.46 (d, J = 4.2 Hz, 20H); UV/Vis (CH_2Cl_2): λ_{max} ($\varepsilon \times 10^{-4}$) = 443 (33.0), 456sh (16.0), 552 (2.0), 591 (1.4), 633 (1.0), 696 nm (1.4 $mol^{-1}dm^3cm^{-1}$); UV/Vis (CH_2Cl_2/HCl): λ_{max} ($\varepsilon \times 10^{-4}$) = 450 (27.9), 482 (13.5), 605 (1.8), 657 (2.4), 720 nm (4.6 $mol^{-1}dm^3cm^{-1}$); emission (CH_2Cl_2): λ = 701 nm; FAB-MS: m/z (%): 593 (100) $[M]^+$; anal. calcd for $C_{41}H_{28}N_4O$: C 83.09, H 4.76, N 9.45; found: C 83.14, H 4.72, N, 9.49.

Dicarbonyl (5,10,15-triphenyl-21-oxacorrolato)rhodium(I) (5): Free-base **4** (0.03 g, 0.057 mmol) was dissolved in alcohol free chloroform (50 mL). Anhydrous sodium acetate (0.047 g, 0.57 mmol) was added to the solution followed by di-μ-chloro-bis[di-carbonyl rhodium(I)] (0.03 g, 0.07 mmol) and the mixture stirred and refluxed for 2 h. The resulting red green solution was filtered through a short silica column eluting with petroleum ether/dichloromethane 10:1 solution. Evaporation of the solvent under reduced pressure gave the product as purple solid (0.02 g, 46 %) which recystallised from dichloromethane/methanol and decomposes above 250 °C. UV/Vis (CH_2Cl_2): λ_{max} ($\varepsilon \times 10^{-4}$) = 420 (13.6), 438sh (9.2), 520 (1.1), 556 (1.41), 581 (0.9) 627 nm (2.1 $mol^{-1}dm^3cm^{-1}$); emission (CH_2Cl_2): λ = 638 nm; anal. calcd for $C_{40}H_{26}Cl_2N_3O_3Rh$: C 62.36, H 3.40, N 5.45; found: C 62.40, H 3.44, N 5.49.

5,10,15-Triphenyl-21-oxacorrolato copper(II) (6): The free-base **4** (0.05 g, 0.095 mmol) and copper chloride (0.16 g, 0.95 mmol) were dissolved in 20 mL of freshly distilled dimethlyformamide (DMF) and refluxed for 2 h. Solvent was evaporated under reduced pressure and column chromatography was done on basic alumina. The reddish green band eluted with dichloromethane was recrystallised with dichloromethane/*n*-heptane gave violet solid (0.031 g, 55 %). UV/Vis (CH_2Cl_2): λ_{max} ($\varepsilon \times 10^{-4}$) = 422 (15.61), 514 (0.82), 552 (0.94), 576 (1.03) 619 nm (2.16 $mol^{-1}dm^3cm^{-1}$); emission (CH_2Cl_2): λ = 637 nm; anal. calcd for $C_{37}H_{23}N_3OCu$: C 75.43, H 3.93 N 7.13; found: C 75.40, H 3.89, N 7.09.

The following metallo corroles such as nickel and cobalt were prepared by similar reactions with nickel chloride and cobalt acetate, respectively:

5,10,15-Triphenyl-21-oxacorrolato nickel(II) (7): Yield: 0.036 g, 65 %; UV/Vis (CH_2Cl_2): λ_{max} ($\varepsilon \times 10^{-4}$) = 398 (7.38), 416 (6.79), 436 (6.65), 606 nm (1.67 $mol^{-1}dm^3cm^{-1}$); emission (CH_2Cl_2): λ = 640 nm; anal. calcd for $C_{37}H_{23}N_3ONi$: C 76.06, H 3.97, N 7.19; found: C 76.02, H 3.92, N 7.15.

5,10,15-Triphenyl-21-oxacorrolato cobalt(II) (8): Yield: 0.027 g, 49 %; UV/Vis (CH_2Cl_2): λ_{max} ($\varepsilon \times 10^{-4}$) = 424 (14.63), 506 (0.75), 556 sh (0.92), 575 (1.12) 618 nm (2.32 $mol^{-1}dm^3cm^{-1}$); emission (CH_2Cl_2): λ = 637 nm; anal. calcd for $C_{37}H_{23}N_3OCo$: C 76.03, H 3.97, N 7.19; found: C 76.08, H 3.93, N 7.16.

Acknowledgements

This work was supported by a grant from the Department of Science and Technology (DST) and Council of Scientific and Industrial Research (CSIR), Government of India, New Delhi, to T.K.C. Support from NSF (grant CHE-9527898) Syracuse University and the W. M. Keck foundation for the purchase of the X-ray instruments to KRS is acknowledged. Use of fluorescence time resolved facility at centre for Ultrafast processes is acknowledged.

[1] S. Licoccia, R. Paolesse, *Struct. Bonding* **1995**, *84*, 71–134.
[2] J. L. Sessler, S. J. Weghorn in *Expanded*, *Contracted and Isomeric Porphyrins*, *Tetrahedron Organic Chemistry Series*, *Vol. 15*, Pergamon, New York, **1997**, pp. 11–125.
[3] A. W. Johnson, R. Price, *J. Chem. Soc.* **1960**, 1649–1653.
[4] A. W. Johnson, I. T. Kay, *Proc. Chem. Soc.* **1961**, 168–169.
[5] A. W. Johnson, I. T. Kay, R. Rodrigo, *J. Chem. Soc.* **1963**, 2336–2342.
[6] a) M. J. Broadhurst, R. Grigg, A. W. Johnson, *J. Chem. Soc. Perkin Trans 1* **1972**, 1124–1135; b) M. J. Broadhurst, R. Grigg, A. W. Johnson, *J. Chem. Soc. Chem. Commun.* **1969**, 23–24.
[7] a) F. Behrens, *Ph.D. Dissertation*, University of Cologne, Germany, **1996**; b) J. Dorr, *Ph.D. Dissertation*, University of Cologne, Germany, **1996**.
[8] a) R. Paolesse, S. Licoccia, M. Fanciullo, E. Morganto, T. Boschi, *Inorg. Chim. Acta* **1993**, *203*, 107–114; b) R. Paolesse, S. Licoccia, G. Bandoli, A. Dolmella, T. Boschi, *Inorg. Chem.* **1994**, *33*, 1171–1176.
[9] E. Rose, A. Kossanyi, M. Quelquejeu, M. Soleilhavoup, F. Duwavran, N. Bernard, A. Lecas, *J. Am. Chem. Soc.* **1996**, *118*, 1567.
[10] a) Z. Gross, N. Galili, I. Saltsman, *Angew. Chem.* **1999**, *111*, 1530–1533; *Angew. Chem. Int. Ed. Engl.* **1999**, *38*, 1427–1429; b) Z. Gross, N. Galili, L. Simkhovich, I. Saltsman, M. Botoshansky, D. Blaser, R. Boese, I. Goldberg, *Org. Lett.* **1999**, *1*, 599–602.
[11] R. Paolesse, L. Jaquinod, D. J. Nurco, S. Mini, F. Sagoni, T. Boschi, K. M. Smith, *Chem. Commun.* **1999**, 1307–1308.
[12] S. J. Narayanan, B. Sridevi, T. K. Chandrashekar, U. Englich, K. Ruhlandt-Senge, *Org. Lett.* **1999**, *1*, 587–590.
[13] B. Sridevi, S. J. Narayanan, A. Srinivasan, M. V. Reddy, T. K. Chandrashekar, *J. Porphyrins Phthalocyanines* **1998**, *2*, 69–78.
[14] T. D. Lash, S. T. Chaney, D. T. Richter, *J. Org. Chem.* **1998**, *63*, 9076–9088.
[15] R. M. Silverstein, G. C. Bassler, T. C. Morrill in *Spectrometric Identification of Organic Compounds*, 5th ed., Wiley, New York, **1991**.
[16] It has been possible to isolate the single crystal of flouride complex of **4** and X-ray structural details will be reported separately.
[17] a) P. J. Chmielewski, L. Latos-Grazynski, M. M. Olmstead, A. L. Balch, *Chem. Eur. J.* **1997**, *3*, 268–278; b) L. Latos-Grazynski, J. Lisowski, M. M. Olmstead, A. L. Balch, *Inorg. Chem.* **1989**, *28*, 1183–1188.
[18] B. Sridevi, S. J. Narayanan, A. Srinivasan, T. K. Chandrashekar, J. Subramanian, *J. Chem. Soc. Dalton Trans.* **1998**, 1979–1984.
[19] S. Will, J. Lex, E. Vogel, H. Schmickler, J. P. Gisselbrecht, C. Haubtmann, M. Bernard, M. Gross, *Angew. Chem.* **1997**, *109*, 367–371; *Angew. Chem. Int. Ed. Engl.* **1997**, *36*, 357–360.
[20] H. R. Harrison, O. J. R. Hodder, D. C. Hodgkin, *J. Chem. Soc.* (*B*) **1971**, 640–645.
[21] a) A. M. Abeysekara, R. Grigg, J. T. Grimshaw, V. Viswanatha, *J. Chem. Soc. Perkin 1* **1977**, 36–44; b) A. M. Abeysekara, R. Grigg, J. T. Grimshaw, T. J. King, *J. Chem. Soc. Perkin 1* **1979**, 2184–2192.
[22] Y. Murakami, Y. Matsuda, K. Sakata, *Inorg. Chem.* **1971**, *10*, 1734.
[23] a) L. Latos-Grazynski, J. Lisowski, M. M. Olmstead, A. L. Balch, *J. Am. Chem. Soc.* **1987**, *109*, 4428; b) J. Lisowski, M. Grzeszczuk, L. Latos-Grazynski, *Inorg. Chim. Acta* **1989**, *161*, 153; c) L. Latos-Grazynski, J. Lisowski, M. M. Olmstead, A. L. Balch, *Inorg. Chem.* **1989**, *28*, 3328.
[24] J. Subramanian, J. H. Fuhrhop, A. Salek, A. Gossauer, *J. Magn. Reson.* **1974**, *15*, 31–39.
[25] W. C. Lin in *The Porphyrins*, *Vol. 4* (Ed.: D. Dolphin), Academic Press, New York, **1979**, pp. 355–375.
[26] J. M. Assour, W. K. Kahn, *J. Am. Chem. Soc.* **1965**, *87*, 207.
[27] N. S. Hush, I. S. Woolsey, *J. Chem. Soc.* **1974**, *3*, 24–34.
[28] V. Balzani, F. Bolletta, M. T. Gondolfi, M. Maestri, *Top. Curr. Chem.* **1978**, *75*, 1.
[29] H. Hope, *Prog. Inorg. Chem.* **1994**, *41*, 1.
[30] SADBS: G. M. Sheldrick, University of Göttingen, Germany, **1996**, using redundant data by the method described by R. H. Blessing, *Acta Crystallogr.* **1995**, *A51*, 33.
[31] G. M. Sheldrick, SHELXL-93, Program for crystal structure solution and refinement, University of Göttingen, Germany, **1993**.
[32] G. M. Sheldrick, SHELXTL-Plus, Program for crystal structure solution and refinement, University of Göttingen, Germany, **1990**.

Received: November 2, 1999 [F2115]